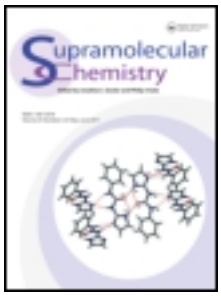

Supramolecular Chemistry
Publication details, including instructions for authors and subscription information:
http://www.tandfonline.com/loi/gsch20

A new diamine containing disiloxane moiety and some derived Schiff bases: synthesis, structural characterisation and antimicrobial activity

Mirela-Fernanda Zaltariov [a], Maria Cazacu [a], Nicoleta Vornicu [b], Sergiu Shova [a], Carmen Racles [a], Mihaela Balan [a] & Constantin Turta [a]

[a] "Petru Poni" Institute of Macromolecular Chemistry, Aleea Gr. Ghica Voda 41A, 700487, Iasi, Romania

[b] Metropolitan Center of Research T.A.B.O.R, The Metropolitanate of Moldavia and Bukovina, Iasi, Romania

Published online: 07 Jun 2013.

To cite this article: Supramolecular Chemistry (2013): A new diamine containing disiloxane moiety and some derived Schiff bases: synthesis, structural characterisation and antimicrobial activity, Supramolecular Chemistry, DOI: 10.1080/10610278.2013.794947

To link to this article: http://dx.doi.org/10.1080/10610278.2013.794947

Supramolecular Chemistry, 2013
http://dx.doi.org/10.1080/10610278.2013.794947

A new diamine containing disiloxane moiety and some derived Schiff bases: synthesis, structural characterisation and antimicrobial activity

Mirela-Fernanda Zaltariov[a], Maria Cazacu[a]*, Nicoleta Vornicu[b], Sergiu Shova[a], Carmen Racles[a], Mihaela Balan[a] and Constantin Turta[a]

[a]*"Petru Poni" Institute of Macromolecular Chemistry, Aleea Gr. Ghica Voda 41A, 700487 Iasi, Romania;* [b]*Metropolitan Center of Research T.A.B.O.R, The Metropolitanate of Moldavia and Bukovina, Iasi, Romania*

(*Received 29 December 2012; final version received 8 April 2013*)

A new siloxane diamine, 1,3-*bis*(amino-phenylene-ester-methylene)tetramethyldisiloxane (**1**), was obtained by a two-step procedure and used to prepare a series of Schiff bases (**2**–**5**), by reaction with different carbonylic compounds: salicylaldehyde, 3,5-dibromosalicylaldehyde, 5-chlorosalicylaldehyde and 3,5-di-*tert*-butyl-2-hydroxybenzaldehyde. All compounds, separated in crystalline form, were characterised by spectral (FTIR, UV–vis and NMR) analysis as well as by single-crystal X-ray diffraction. In these structures, different packing motifs occur depending on the different association degree determined by intra- and intermolecular $\pi-\pi$ stacking interactions. Antimicrobial activity of the compounds was evaluated against three fungi and two bacteria, where the Schiff bases derived from salicylaldehyde and in special 5-chlorosalicylaldehyde showed remarkable activity.

Keywords: Schiff base; amine; siloxane; supramolecular structure; self-assembling

1. Introduction

A large variety of carbonylic and amine compounds can be used to prepare azomethines (*1*, *2*). The synthetic flexibility permits to design molecular structures with tunable properties (chemical, optical, magnetic and electrical) and numerous representative derivatives found a wide variety of applications in many fields such as medicine (to design medicinal compounds) (*3*), biology (as biochemical and antimicrobial reagents due to similarities with natural biological compounds) (*4*), analytical chemistry (reagents or optical, electrochemical and chromatographic sensors) (*5*, *6*) and materials chemistry (catalysts and antimicrobial reagents, light emitting diodes OLED, PLED) (*7*), or as oxygen carriers (*8*). Schiff base compounds are among the most used ligands playing an important role in the development of coordination chemistry. The main reasons for this position are their easy preparation and coordination ability with a large variety of metals with different oxidation states forming highly stable coordination compounds (*9*–*11*). The lone electron pair in a sp^2 hybridised orbital of nitrogen atom of the azomethine group imparts excellent chelating ability especially when there are one or more donor atoms close to the azomethine group (*10*). Depending on the chosen amine, the salen-type metal complexes can conformationally be more rigid or flexible, the last being able to adopt a variety of geometries and to generate various active-site environments for the different oxidation reactions. This flexibility, similar to that observed in metalloproteins, is a key factor for the biomimetic activity of these molecules (*12*). Therefore, although there are an extremely large number of publications on Schiff bases (*13*) and their metal complexes (*14*), there is still intensive research in this area which mainly aims to diversify the range of amines and aldehydes and exploit the full potential offered by this class of compounds. In the last decade, we have prepared small molecule or polymeric azomethines based on different carbonylic derivatives and a siloxane diamine, mainly 1,3-*bis*(3-aminopropyl)tetramethyldisiloxane (*15*–*20*). The presence of the tetramethyldisiloxane moiety with its large and flexible Si—O—Si bond angle ranging between 135° and 180° might confer some special features such as, low glass and melt transitions or self-assembling ability.

Although it might be of interest, this direction was insufficiently explored until now. A relatively small number of compounds of this type are reported in the literature due to the difficulty in their characterisation (*21*–*23*). Highly flexible siloxane bonds make them difficult to investigate by single-crystal X-ray diffraction.

In this study, we have synthesised an original siloxane diamine and four derived Schiff bases by its reaction with salicylaldehyde, 3,5-dibromosalicylaldehyde, 5-chlorosalicylaldehyde and 3,5-di-*tert*-butyl-2-hydroxybenzaldehyde. The compounds were characterised by spectral (FTIR, UV and NMR) analysis as well as by single-crystal X-ray diffraction. Antimicrobial activity against several species was also evaluated.

*Corresponding author. Email: mcazacu@icmpp.ro

2. Results and discussion

A siloxane-containing diamine was prepared by a two-step procedure consisting of synthesis and isolation of sodium salt of *p*-aminobenzoic acid (Scheme 1(a)) followed by the esterification with bifunctional halo-compound containing siloxane moiety, 1,3-*bis*(chlormethyl)-1,1,3,3-tetramethyl-disiloxane (Scheme 1(b)). The first step occurred in an aqueous reaction medium, whereas the second step occurred in DMF.

The salt formation (Figure S1(a) of the Supplementary Information, available online) was verified by FTIR spectroscopy where the band at 1664 cm^{-1} characteristic for the carboxylic group of *p*-aminobenzoic acid disappeared being replaced by a new strong band at 1537 cm^{-1} assigned to the carboxylate group. In the FTIR spectrum of the condensation product (Figure S1(b) of the Supplementary Information, available online), there are present the absorption bands characteristic of the primary aromatic amine at 3433, 3352 and 3236 cm^{-1}, besides those for ester group at 1697 cm^{-1}, and for dimethylsiloxane moiety at 1074 cm^{-1} (Si—O—Si), 843 and 1257 cm^{-1} (Si—CH_3). In the ^{1}H NMR spectrum of the diamine (Figure S2 of the Supplementary Information, available online), the signals of aromatic protons appear at 7.84 and 6.66 ppm, whereas the peak corresponding to resonance of the amine protons appear at 4.09 ppm. Other peaks are those at 0.21 and 3.94 ppm corresponding to the protons from Si—CH_3 and Si—CH_2, respectively. Their intensity ratios (Ar: —NH_2: Si—CH_3: Si—CH_2 = 2:1:3:1) correspond to the presumed structure. In the ^{13}C NMR spectrum (Figure S3 of the Supplementary Information, available online), the —C═O peak appears at 167.3 ppm, the aromatic carbons appear between 113.8 and 150.7 ppm, the —CH_2—Si peak is present at 57.4 ppm and the CH_3—Si peak appears at − 0.8 ppm. The 2D NMR spectra used for the assignment of the signals from the 1D NMR spectra of compound **1** are shown in Figures S4–S6 of the Supplementary Information, available online.

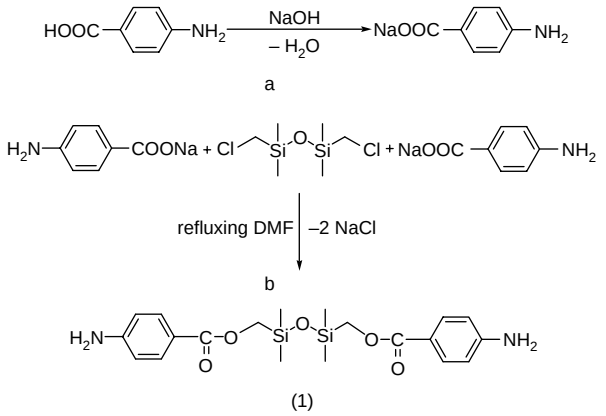

Scheme 1. Two-step synthesis pathway leading to siloxane diamine **1**.

All syntheses of the Schiff base compounds were performed under similar conditions by condensation of diamine 1 with four differently substituted salicylaldehyde derivatives in 1:2 molar ratio, according to Scheme 2.

Condensation of the aldehydes with primary amine readily gave the corresponding imines, which were easily identified by their IR and ^{1}H NMR spectra. Thus, fourier transform infrared (FT-IR) spectra of the imines show characteristic absorption bands attributed to the azomethine bond (—CH═N—) at 1620 cm^{-1} (**2**), 1616 cm^{-1} (**3**) and 1618 cm^{-1} (**4** and **5**), siloxane bond (—Si—O—Si—) at 1055–1072 cm^{-1}, Si—CH_3 at 837–842 cm^{-1} and 1249–1255 cm^{-1}, and (νC═O) in the ester group at 1706–1720 cm^{-1} (Figure S7 of the Supplementary Information, available online). The ^{1}H NMR spectra of all the Schiff bases indicate the formation of the azomethine bond by the presence of the peak corresponding to —CH═N— proton at 8.68 ppm (**5**), 8.57 ppm (**4**), 8.56 ppm (**3**) and 8.64 ppm (**2**), and specific aromatic protons from diamine and aldehyde moieties with some modifications compared with the starting compounds. The peaks corresponding to proton resonance from tetramethyldisiloxane units appear at 0.30–0.25 ppm and that assigned to —CH_2— at 4 ppm in the intensity ratio corresponding to the presumed structures. All the 1D and 2D NMR experiments used for the characterisation of compounds **2**–**5** are shown in Figures S8–S27 of the Supplementary Information, available online.

The imines prepared in this way were formed in good yields and were of high purity, as single crystals. All compounds are stable at room temperature in the solid state.

2.1 Crystal structure

Compound **1** has a molecular crystal structure composed from neutral entities, as depicted in Figure 1. The main crystal structure motif can be characterised as a two-dimensional layer (Figure 2). The construction of these layers occurs via a system of N1—H···O1 hydrogen bonds, the formation of which is completely realised in the crystal. The hydrogen bonds parameters are presented in Table 1. The further extension of the supramolecular architecture occurs through N2—H···O5($1 + x$, y, z) hydrogen bond, so that the crystal structure results from the packing of two-dimensional double layers, the view of which is shown in Figure 3.

The X-ray molecular structure of compound **2** is presented in Figure 4, whereas those for compounds **3** and **4** are provided in the supporting information (Figures S28 and S29 of the Supplementary Information, available online).

The asymmetric part of the unit cell in the crystal structure of **3** and **4** contains two discrete molecules (denoted as A and B) as crystallographic independent

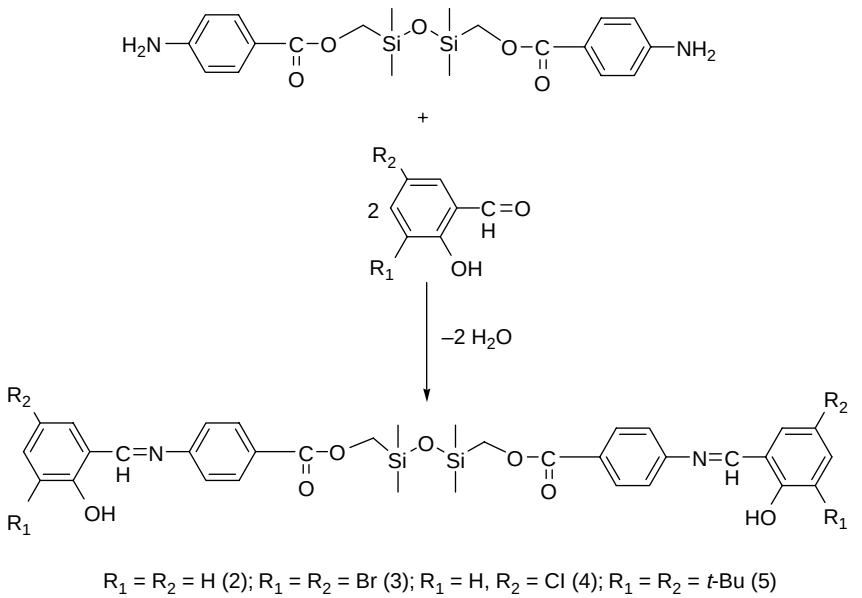

$R_1 = R_2 = H$ (2); $R_1 = R_2 = Br$ (3); $R_1 = H$, $R_2 = Cl$ (4); $R_1 = R_2 = t$-Bu (5)

Scheme 2. Reaction pathway for the synthesis of the Schiff bases, **2**–**5**.

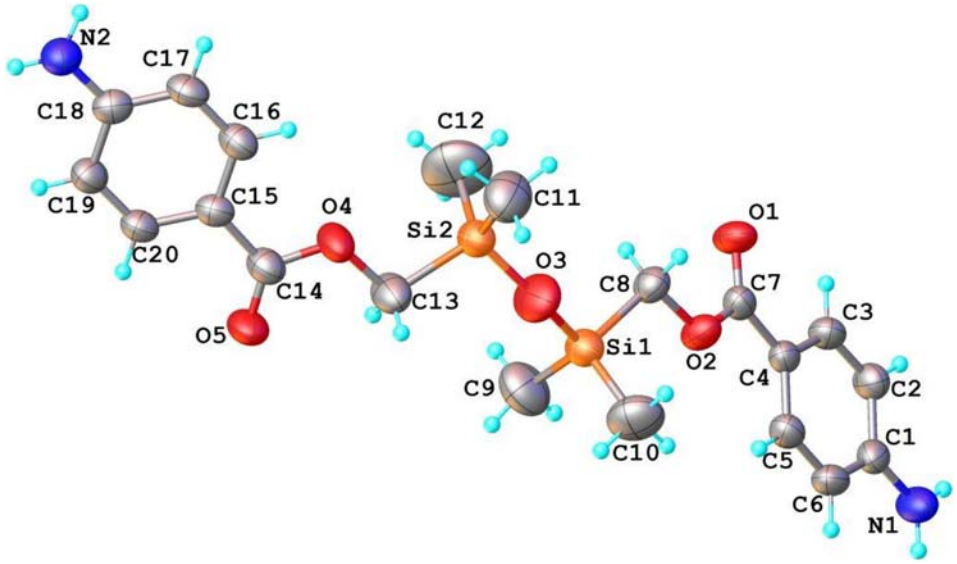

Figure 1. X-ray molecular structure of compound **1**. Thermal ellipsoids are drawn at 50% probability level.

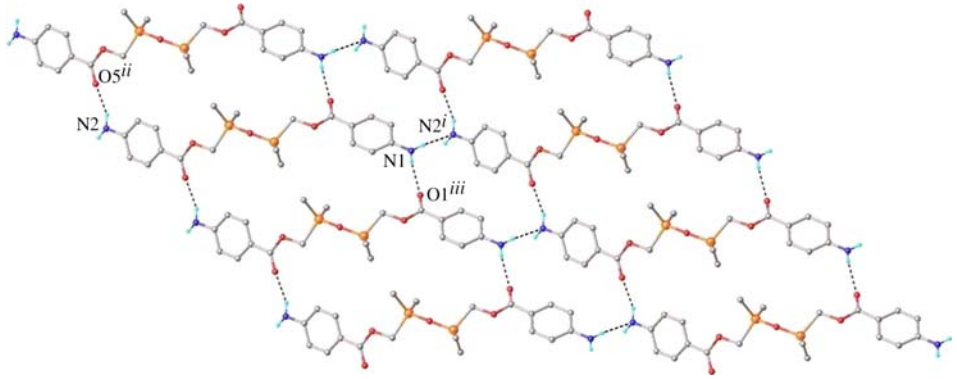

Figure 2. The association of the molecules **1** through N–H···O hydrogen bonds in the crystal.

Table 1. H-bonds parameters.

	Distance (Å)				
D—H···A	D—H	H···A	D···A	Angle D—H···A (°)	Symmetry code
1					
N1—H···O1	0.86	2.18	2.960(3)	150.4	$x-1, y, z$
N1—H···N2	0.86	2.35	3.187(3)	164.2	$x-2, 1+y, z-1$
N2—H···O1	0.85	2.45	3.124(1)	136.8	$1-x, 1-y, 1-z$
N2—H···O5	0.86	2.13	2.938(3)	156.6	$1+x, y, z$
2					
O1—H···N1	0.82	2.21	2.617(8)	149.5	x, y, z
O7—H···N2	0.82	1.93	2.594(6)	137.6	x, y, z
3					
O1A—H···N1A	0.82	1.88	2.600(5)	146.1	x, y, z
O7A—H···N2A	0.82	1.85	2.573(4)	147.2	x, y, z
O1B—H···N1B	0.82	1.88	2.586(4)	142.9	x, y, z
O7B—H···N2B	0.82	1.85	2.584(5)	147.8	x, y, z
4					
O1A—H···N1A	0.90	1.79	2.631(5)	154.7	x, y, z
O7A—H···N2A	0.91	1.79	2.595(6)	145.6	x, y, z
O1B—H···N1B	0.90	1.81	2.614(6)	147.2	x, y, z
O7B—H···N2B	0.92	1.82	2.589(7)	140.2	x, y, z
5					
O1—H···N1	0.82	1.83	2.568(4)	148.4	x, y, z
O1X—H···N1X	0.82	1.88	2.57(2)	140.8	x, y, z

units, which exhibit similar geometric parameters. Structural studies have revealed that in all studied structures, the molecules are in *cis* conformation, the aromatic rings being oriented on the same side with respect to siloxane moiety. The hydroxyl groups act as donor in H-bonding towards azomethine nitrogen as acceptor (Table 1). The molecular conformation for **2**, **3** and **4** is determined by intramolecular $\pi-\pi$ stacking interaction,

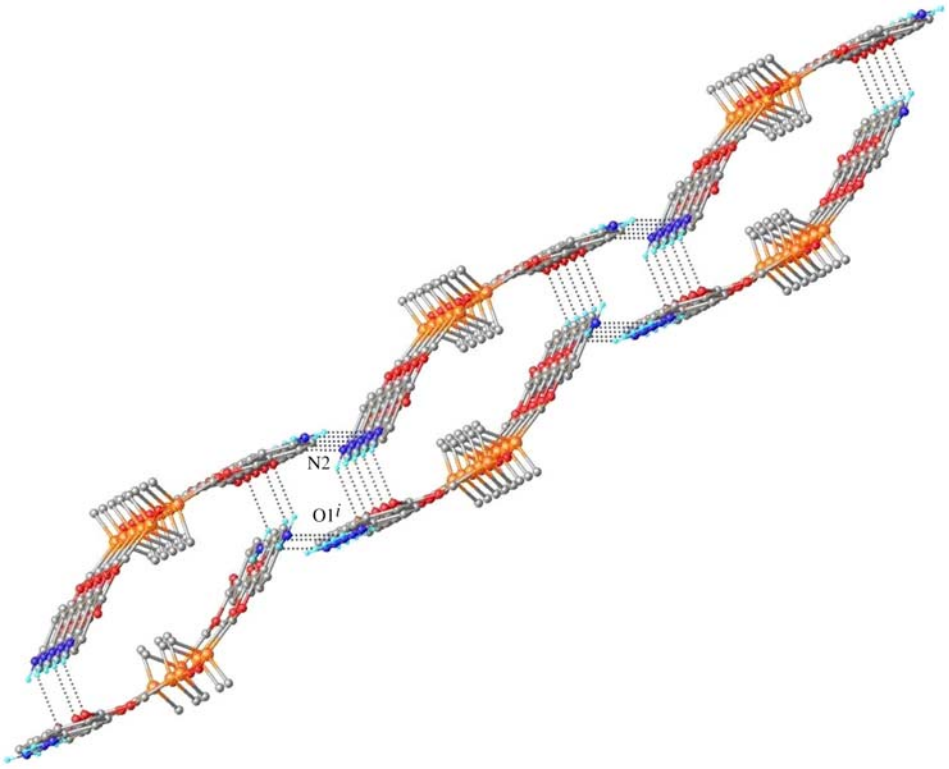

Figure 3. The view of two-dimensional supramolecular double layer in the crystal structure **1**.

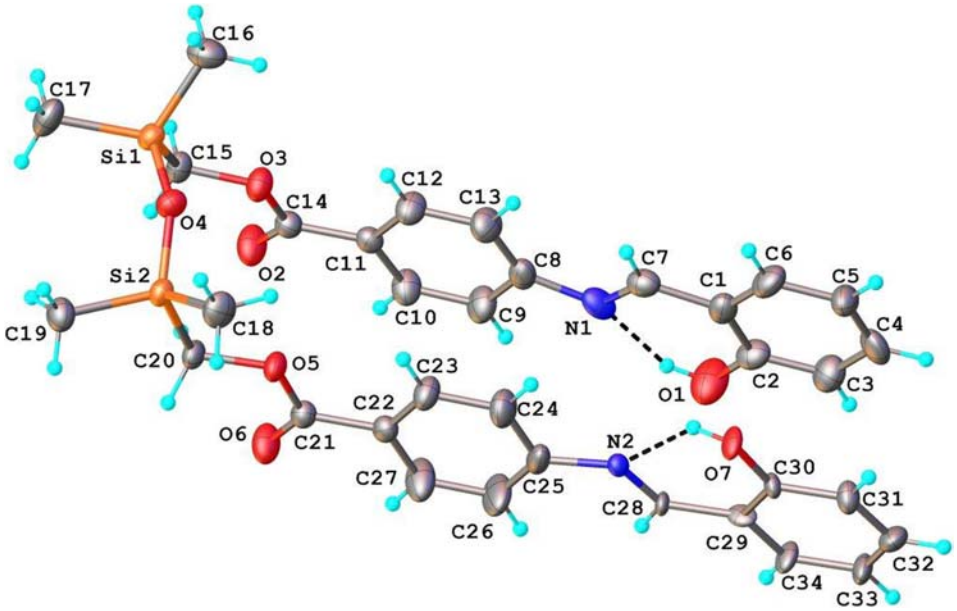

Figure 4. Molecular structure (40% probability ellipsoids) of compound **2**.

which is evidenced by short interplanar spacing between adjacent aromatic systems (Figures 4, S28 and S29 of the Supplementary Information, available online, respectively). The steric effect of *t*-butyl substitutes in **5** imposes the changes in molecular conformation leading to the large separation of the aromatic rings and the absence of the π−π stacking interaction within the molecule (Figure 5).

At the same time, the intermolecular π−π stacking interactions play the key role in the crystal structure formation for compounds **2**–**5**. Figures 6–9 show the packing diagram for crystal structures **2**–**5**. Compounds **2** (Figure 6) and **4** (Figure 8) have a similar crystal structure motif, which results from the packing of the isolated bi-molecular entities associated by intermolecular π−π

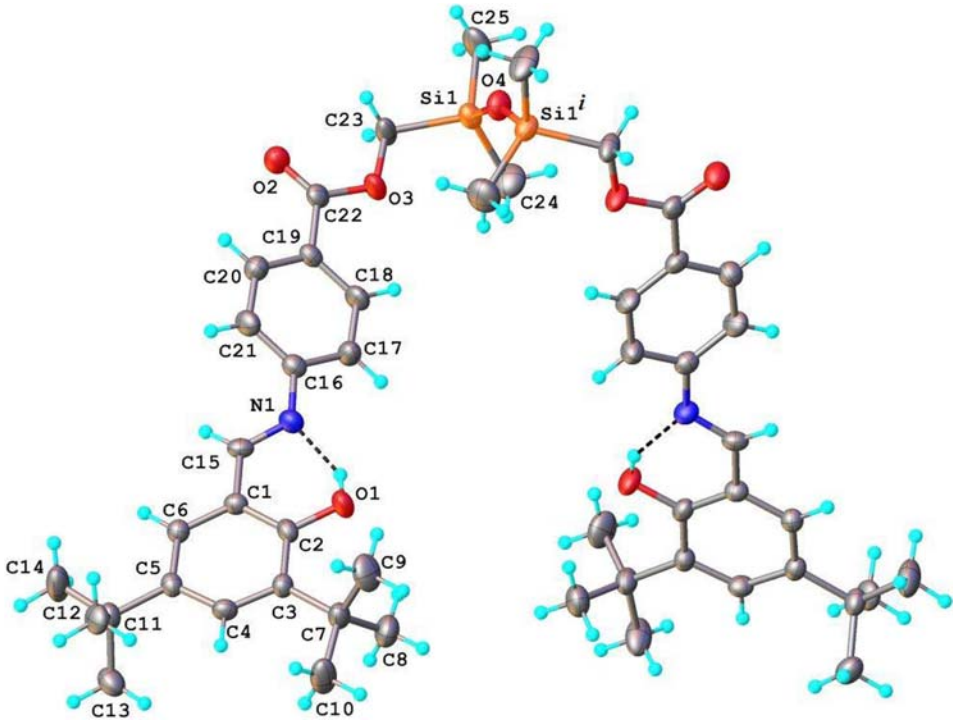

Figure 5. Molecular structure (50% probability ellipsoids) of compound **5** with special position for O4 atom on two-fold axis.

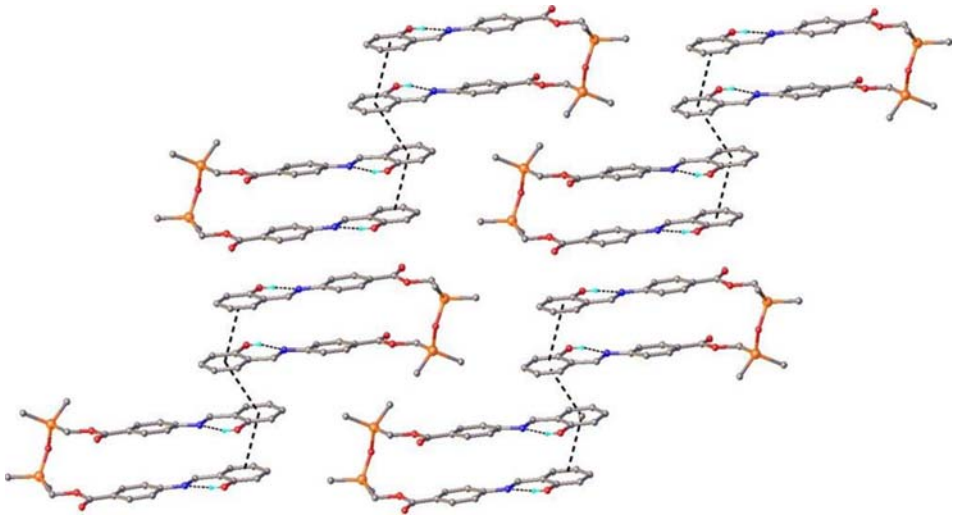

Figure 6. View of the crystal structure **2**. H-atoms are omitted for clarity. Centroid-to-centroid distances are in the range between 3.751 and 3.868 Å.

stacking interaction. On the contrary, the crystal structure of compound **3** (Figure 7) is characterised by the parallel packing of two-dimensional double layers, whereas compound **5** (Figure 9) is packed as one-dimensional supramolecular chains.

The values of Si—O—Si angles and Si—O distances for compounds **2**–**5** are in the range between 143.91–172.3° and 1.526–1.638 Å, respectively (Table 2).

2.2 UV–vis spectroscopy

The absorption spectra of the amine and derived Schiff bases recorded in DMF are presented in Figure 8. The UV data are centralised in Table 3 where the extinction coefficients at the maximum absorption peaks are also presented.

As it can be seen, while the diamine spectrum exhibits one absorption peak at 294 nm characteristic for $\pi-\pi*$

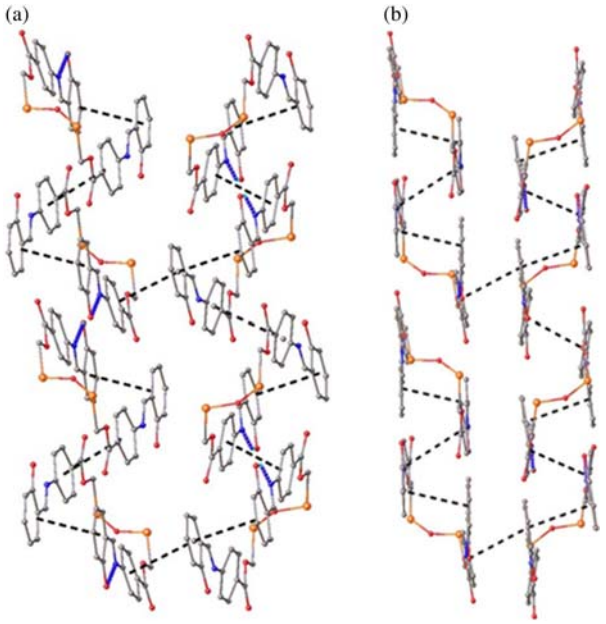

Figure 7. Views of two-dimensional double layer in the crystal structure **3**. H-atoms are omitted for clarity. Centroid-to-centroid distances are in the range between 3.703 and 4.042 Å.

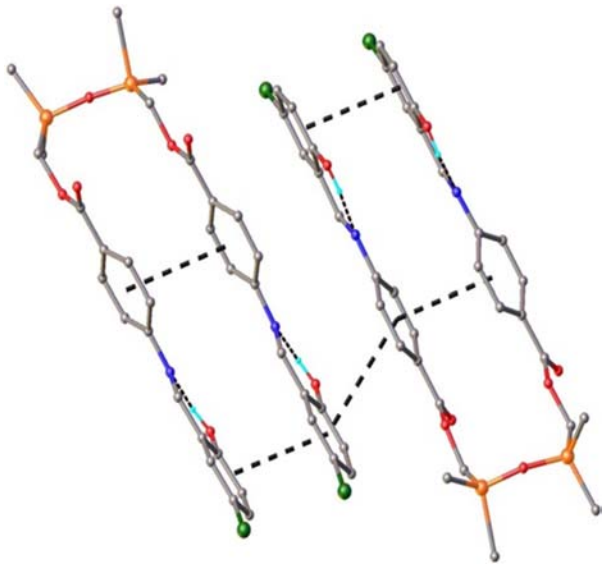

Figure 8. $\pi-\pi$ stacking association in crystal structure **4**. H-atoms are omitted for clarity. Centroid-to-centroid distances are in the range between 3.761 and 4.096 Å.

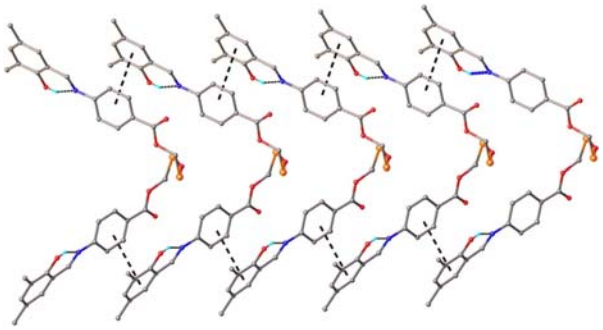

Figure 9. $\pi-\pi$ stacking one-dimensional chain in the crystal structure **5**. H-atoms are omitted for clarity. Centroid-to-centroid distance is equal to 4.096 Å.

transition in aromatic rings, the Schiff bases exhibit two absorption peaks, attributed to $\pi-\pi*$ transitions in aromatic ring (at 282–306 nm) and azomethine groups (at 340–362 nm). The position of these bands differs slightly from each other being probably influenced by the substituent type at the aromatic ring. In the case of the compound **3**, a supplementary large band appears at 426 nm which, according to the literature (*24*), should be assigned to the intramolecular charge transfer involving the whole molecule. As mentioned earlier, as compared with the other Schiff bases compounds (**2**, **4** and **5**), compound **3** forms, beside the intramolecular, the most extensive intermolecular $\pi-\pi$ interactions resulting into the formation of two-dimensional double layers (Figure 7(a),(b)). This could be why UV–vis spectrum is different (Figure 10(a)). Moreover, the spectrum is influenced by the nature of the solvent as can be seen in Figure 10(b). Thus, in a less polar solvent such as CH_2Cl_2, where the intermolecular interactions could be favoured, the maximum of this absorption band slightly shifts to higher wavelength value (433 nm) but significantly decreases in intensity, from 4700 $M^{-1}\,cm^{-1}$ in DMF to 2113 $M^{-1}\,cm^{-1}$ in CH_2Cl_2 (Table 3).

Table 2. Si—O—Si bond angles and bond distances for all the molecules.

			3		**4**		
Parameter	**1**	**2**	A	B	A	B	**5**
Si—O length	1.614(2); 1.608(2)	1.624(2); 1.637(2)	1.623(3); 1.628(3)	1.625(3); 1.638(3)	1.577(3); 1.600(3)	1.603(3); 1.526(3)	1.629(1)
Si—O—Si angle	158.1(2)	147.4(1)	146.5(2)	143.9(2)	158.9(2)	172.0(3)	153.8(3)

Table 3. UV–vis absorption data for the synthesised ligands.

Sample	Solvent	Molar concentrations (mol/L)	λ_{max}, nm (ε, $M^{-1}\,cm^{-1}$)	
1	DMF	4×10^{-5}	296 (39,030)	–
2	DMF	3×10^{-5}	282 (22,800)	344 (18,730)
3	DMF	2×10^{-5}	296 (47,400)	330sh (5395), 426 (4700)
	CH_2Cl_2	3.9×10^{-5}	280 (24,460)	335 (3693), 433 (2113)
4	DMF	2×10^{-5}	294 (39,010)	350 (22,630)
5	DMF	2×10^{-5}	306 (25,400)	362 (15,550)

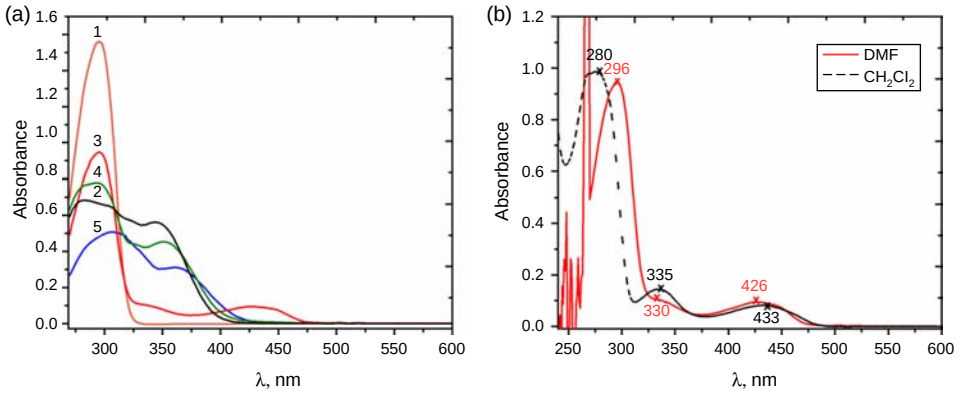

Figure 10. UV–vis spectra of the compounds registered in DMF solution – a; comparative UV–vis spectra of compound **3** registered in DMF and CH_2Cl_2 – b.

Table 4. Results of *in vitro* antimicrobial and antifungal activity testing of compounds **2**, **3**, **4** and **5**.

	MIC (μg/ml)[a]				
Sample	*A. niger*	*P. frequentans*	*A. alternata*	*P. aeruginosa*	*Bacillus* sp.
2	0.8	0.8	0.9	1	1
3	>128	>128	>128	>128	>128
4	0.05	0.05	0.06	0.1	0.1
5	>128	>128	>128	>128	>128
Control plates[b]	>3	>3	>3	>3	>3

[a] Minimum inhibitory concentration.
[b] Based on solvent only.

2.3 Antimicrobial activity

It has already been proved in numerous publications (*25–27*) that the Schiff bases and their metal complexes show a wide range of biological activities, such as antitumoural (*25*), antiviral (*26*) or antimicrobial (*27*). The azomethine group present in such compounds has been shown to be essential for biological activity (*28*, *29*). For the new Schiff bases obtained in this paper, we assessed antifungal and antibacterial activity *in vitro* using three fungi species (*Aspergillus niger*, *Penicillium frequentans* and *Alternaria alternata*) and two bacteria – Gram-negative (*Pseudomonas aeruginosa*) and Gram-positive bacteria (*Bacillus*). The experimental test results on compounds were compared against DMF as the control and are expressed by value of the minimum inhibitory concentration (MIC, μg/ml) in Table 4.

According to these results, compounds **3** and **5** derived from 3,5-dibromosalicylaldehyde and 3,5-di-*tert*-butyl-2-hydroxybenzaldehyde, respectively, had no effect against tested fungi and bacteria (MIC > 128 μg/ml). Instead, Schiff base 4, derived from 5-chlorosalicylaldehyde, proved to have the greatest potential for biological activity. MIC values for this compound range from 0.05 to 0.1 μg/ml revealing high antimicrobial effect compared with control plate. This could be attributed to the presence of chlorine in position 5, which, due to its electron-acceptor effect, polarises the azomethine groups more than do other substituents (*27a*). The combination of our diamine, 1,3-bis(amino-phenylene-ester-methylene)tetramethyldisiloxane, with salicylaldehyde as in compound **2**, has a lower inhibitory effect on micro-organisms than compound **4**. However, the found MIC values between 0.8 and 1 μg/ml reveals some antimicrobial effect of the compound **2** in comparison with the control.

3. Conclusions

A new diamine containing disiloxane moiety, 1,3-*bis*(amino-phenylene-ester-methylene)tetramethyldisiloxane, has been prepared and fully characterised. Structural analysis by single-crystal X-ray diffraction revealed its self-assembling in 3D structure through N—H···O and N—H···N hydrogen bonds. By condensation reaction of this diamine with salicylaldehyde and its derivatives, 3,5-dibromosalicylaldehyde, 5-chlorosalicylaldehyde and 3,5-di-*tert*-butyl-2-hydroxybenzaldehyde, the corresponding *bis*(2-hydroxyazomethine)s **2**–**5** have been obtained. All the compounds were characterised by spectral methods (FTIR and NMR spectroscopy) and their crystal structures were studied by X-ray crystallography. All compounds have a molecular crystal structure, but exhibit different crystal packing motifs. Thus, compounds **2** and **4** show intra- and intermolecular π–π interactions between aromatic rings, which determined the formation of isolated di-molecular associates in the crystal structure. In compounds **3** and **5**, both intramolecular and extended intermolecular π–π interactions occur resulting in two-dimensional double layers and one-dimensional chains, respectively. The optical behaviour is influenced by the electronic nature of the group appended to the aromatic ring but also by the type of the interactions occurring within the molecule and at intermolecular level, as was emphasised by UV–vis spectra. The results of the antifungal and antibacterial activities test recommend two of the new azomethines synthesised as potential antimicrobial agents.

4. Experimental

4.1 Materials

p-Aminobenzoic acid (Aldrich), 1,3-*bis*(chlormethyl)-1,1,3,3-tetramethyldisiloxane (Fluka, Chemie GmbH, Steinheim, Germany), salicylaldehyde, 3,5-dibromosalicylaldehyde, 5-chlorosalicylaldehyde and 3,5-di-*tert*-buthyl-2-hydroxybenzaldehyde (Sigma-Aldrich, Chemie GmbH, Steinheim, Germany), methanol (Chimopar, Bucuresti, Romania), chloroform (Chimopar), dimethylformamide (Aldrich), diethyl ether (Aldrich) and acetonitrile (Aldrich) were used as received.

Three fungi (*A. niger* ATCC 53346, *P. frequentans* ATCC 10110, *Alternaria alternata* ATCC 8741) from pure culture and two bacteria (*Pseudomonas aeruginosa* ATCC 27813 and *Bacillus* sp. ATCC 15970) species from American Type Culture Collection (ATCC), USA, were used for biological activity testing. Petri plates with agar culture medium type –Sabouraud (Merck, Darmstadt, Germany) were used for these measurements.

4.2 Spectral techniques

FT-IR spectra were recorded using a Bruker Vertex 70 FT-IR spectrometer. Registrations were performed in the transmission mode in the range of 400–4000 cm^{-1} at room temperature with a resolution of 2 cm^{-1} and accumulation of 32 scans.

The NMR spectra were recorded on a Bruker Avance DRX 400 MHz Spectrometer (Bruker, Rheinstetten, Germany) equipped with a 5 mm QNP direct detection probe and *z*-gradients. Spectra were recorded in $CDCl_3$ at room temperature. The chemical shifts are reported as δ values (ppm). The atom labelling for the NMR assignments is that from XRD structures. The assignments of all the signals in the 1D NMR spectra were done using 2D NMR experiments such as H,H-COSY, H,C-HMQC and H,C-HMBC.

UV–vis absorption spectra measurements were carried out in DMF solution on a Specord 200 spectrophotometer (Analytik Jena AG, Jena, Germany).

4.3 Antimicrobial activity

In vitro antimicrobial activity tests against the bacterial species *P. aeruginosa* and *Bacillus* sp., and fungal species *A. niger*, *P. frequentans* and *A. alternata*, were carried out according to the standard procedures (SR-EN 1275:2006 and NCCLS:1993) on agar-type media by the disc diffusion method. According to these procedures, the successive dilutions have been made to obtain the suspensions of micro-organisms. Final load of as prepared stock inoculum was 1×10^{-4} μg/ml. Culture was performed by using mixture 1:1 micro-organism suspension and solution of the compound to be tested that were deposed on the disc and solid medium. Solutions of 0.5, 1.0 and 1.5 wt% sample concentration in DMF have been prepared for each compound and soaked in filter paper disc of 5 cm diameter and 1 mm thickness. The discs were placed on the previously seeded plates and incubated at 32°C. A blank sample was also prepared in order to verify the influence of the solvent on the biological activity. The diameter of inhibition zone around each disc was measured after 48 h and after 7 days. The antimicrobial activity was estimated by measuring the diameter of the area inhibited by the tested compounds.

4.4 Crystallography

Crystallographic measurements for compounds **1**–**5** were carried out with an Oxford-Diffraction XCALIBUR E CCD diffractometer (Oxford Diffraction Limited, Oxford, UK) equipped with graphite-monochromated Mo Kα radiation. The crystals were placed 40 mm from the CCD detector. The unit cell determination and data integration were carried out using the CrysAlis package of Oxford Diffraction (*30*). All structures were solved by direct methods using SHELXS-97 (*31*), and refined by full-matrix least-squares on Fo^2 with SHELXL-97 (*31*). All atomic displacements for non-hydrogen, non-disordered atoms were refined using an anisotropic model. In structure **4**, disiloxane methyl groups and the atoms of both salicylimine moieties in structure **2** presented too large thermal ellipsoids, so that disordered models, in combination with the available tools (PART, DFIX and SADI) of SHELXL97 were applied in order to better fit the electron density. The combined anisotropic/isotropic refinement has been used for these non-H atoms. All the asymmetric parts of the unit cell in structure **5** were found to be statistically disordered over two positions with 0.72 and 0.28 s.o.f. Nevertheless, anisotropic approach could be applied for both major and minor components. Hydrogen atoms have been placed by Fourier Difference accounting for the hybridisation of the supporting atoms and the possible presence of hydrogen bonds in the case of donor atoms. The main crystallographic data together with refinement details are summarised in Table 5.

4.5 Procedure

4.5.1 Synthesis of p-aminobenzoic acid sodium salt

NaOH (1.2 g, 0.03 mol) was dissolved in 10 mL of distilled water and then 4.11 g (0.03 mol) *p*-aminobenzoic acid was added. After complete dissolution of the *p*-aminobenzoic acid, the water was evaporated and the yellow powder obtained was dried in oven at 80°C for 2 h. The resulting sodium salt (4.3 g, 90% yield) was first analysed by IR spectroscopy.

4.5.2 Synthesis of the siloxane-containing diamine, 1,3-bis(amino-phenylene-ester-methylene)tetramethyldisiloxane, **1**

In a round-bottom flask equipped with reflux condenser having attached a calcium chloride tube and magnetic stirrer, 30 mL of dry dimethylformamide, 4.3 g (0.027 mol) *p*-aminobenzoic acid sodium salt and 3.12 g (2.2 mL, 0.0135 mol) of 1,3-*bis*(chloromethyl)-1,1,3,3 tetramethyldisiloxane were added. The reaction mixture was stirred under argon atmosphere to reflux for 8 h. The NaCl by-product was separated by filtration and the filtrate was poured into 100 mL of distilled water, when a brown solid as a resin separated on the glass bottom. After removing liquid phase, the residue was washed with water, dried and dissolved in chloroform. The organic solution was extracted several times with water until this resulted colourless. The organic phase was evaporated and dried to afford a crude residue that was crystallised from chloroform obtaining colourless crystals (3.88 g, 33% yield).

Table 5. Crystallographic data, details of data collection and structure refinement parameters for **1**–**5**.

	1	**2**	**3**	**4**	**5**
Empirical formula	$C_{20}H_{28}N_2O_5Si_2$	$C_{34}H_{36}N_2O_7Si_2$	$C_{34}H_{32}Br_4N_2O_7Si_2$	$C_{34}H_{34}Cl_2N_2O_7Si_2$	$C_{50}H_{68}N_2O_7Si_2$
Formula weight	432.62	640.83	956.44	709.71	865.24
Temperature (K)	200	200	200	293	200
Crystal system	Triclinic	Triclinic	Triclinic	Triclinic	Monoclinic
Space group	*P*-1	*P*-1	*P*-1	*P*-1	*C*2/c
a (Å)	8.7629(17)	8.623(2)	13.1841(4)	12.3071(13)	33.8631(15)
b (Å)	10.603(2)	12.4417(11)	16.3416(6)	16.4867(18)	6.7706(6)
c (Å)	14.399(3)	16.1316(16)	18.0840(6)	19.2999(16)	27.1232(14)
α (°)	74.241(17)	97.304(8)	95.577(3)	104.807(8)	90.00
β (°)	80.868(16)	93.155(13)	107.268(3)	100.962(8)	128.530(7)
γ (°)	68.356(18)	108.928(14)	94.349(3)	101.125(9)	90.00
V (Å^3)	1194.3(4)	1615.2(4)	3680.4(2)	3594.5(6)	4864.7(5)
Z	2	2	4	4	4
D_{calc} (mg/mm^3)	1.203	1.318	1.726	1.311	1.181
μ (mm^1)	0.179	0.161	4.488	0.295	0.124
Crystal size (mm^3)	0.15 × 0.15 × 0.05	0.15 × 0.1 × 0.1	0.2 × 0.2 × 0.1	0.1 × 0.05 × 0.05	0.2 × 0.1 × 0.1
θ_{min}, θ_{max}(°)	5.02–52°	5.02–52°	4.76–52°	4.88–52°	4.82–52°
Reflections collected	9388	11353	27605	26765	34097
Independent reflections	4692[R_{int} = 0.0211]	6352[R_{int} = 0.0226]	14,471[R_{int} = 0.0460]	14,107[R_{int} = 0.0589]	4781[R_{int} = 0.0556]
Data/restraints/parameters	4692/0/266	6352/18/524	14471/0/891	14107/0/870	4781/87/558
GOF[a]	1.052	1.051	0.990	0.931	1.085
R_1[b] (I(2σ(I)	0.0541	0.0526	0.0559	0.0864	0.0785
wR_2[c] (all data)	0.1366	0.1371	0.0886	0.1308	0.1965
Largest diff. peak/hole (e Å^{-3})	0.39/–0.19	0.36/–0.27	1.57/–0.74	0.31/–0.24	0.23/–0.22

[a] $GOF = \{\Sigma[w(F_o^2 - F_c^2)^2]/(n-p)\}^{1/2}$, where n is the number of reflections and p is the total number of parameters refined.
[b] $R_1 = \Sigma||F_o|-|F_c||/\Sigma|F_o|$.
[c] $wR_2 = \{\Sigma[w(F_o^2 - F_c^2)^2]/\Sigma[w(F_o^2)^2]\}^{1/2}$.

IR ν_{max} (KBr), cm^{-1}: IR ν_{max} (KBr), cm^{-1}: 3433 m, 3352 s, 3236 m, 2957 w, 2907 w, 1695 vs, 1643 s, 1599 vs, 1514 s, 1441 m, 1410 w, 1315 vs, 1302 vs, 1254 s, 1171 s, 1117 s, 1074 s, 955 w, 843 s, 798 s, 771 s, 729 w, 700 m, 635 w, 604 m, 505 m, 393 w. ^{1}H NMR ($CDCl_3$, 400.13 MHz, δ, ppm): 7.86 (d,$^3J_{H,H}$ = 8.4 Hz, 4H, H3,5,16,20), 6.66 (d,$^3J_{H,H}$ =8.4 Hz, 4H, H2,6,17,19), 4.09 (s, 4H, NH_2), 3.94 (s, 4H, H8,13), 0.21 (s, 12H, H9-12). ^{13}C NMR ($CDCl_3$, 100.16 MHz, δ, ppm): 167.3 (C7,17), 150.67 (C1,18), 131.4 (C3,5,16,20), 120.0 (C4,15), 113.8 (C2,6,17,19), 57.4 (C7,14), − 0.8 (C9-12).

4.5.3 Synthesis of Schiff bases

*4.5.3.1 Synthesis of the imine **2** derived from the diamine **1** and salicylaldehyde*. To a stirred solution of diamine, **1**, (0.432 g, 1 mmol) in methanol/chloroform (1:2, v/v), freshly distilled salicylaldehyde (0.244 g, 0.21 mL, 2 mmol) was added and the mixture was stirred at room temperature for 3 h. A yellow precipitate was formed. The product was filtered, washed with diethyl ether and then crystallised from acetonitrile (0.58 g, 90% yield). IR ν_{max} (KBr), cm^{-1}: 3415 vw, 3060 w, 2958 w, 2906 w, 2854 vw, 1720 vs, 1620 s, 1598 vs, 1571 s, 1523 w, 1506 w, 1492 m, 1454 m, 1415 m, 1384 w, 1361 m, 1319 vs, 1292 s, 1280 s, 1249 vs, 1186 m, 1172 s, 1149 s, 1110 s, 1056 vs, 1012 m, 968 w, 958 w, 910 w, 850 s, 837 s, 800 s, 771 s, 752 s, 731 m, 690 m, 663 w, 634 w, 597 w, 557 w, 516 m, 443 w, 397 m.

^{1}H NMR ($CDCl_3$, 400.13 MHz, δ, ppm): 12.93 (s, 2H, OH), 8.64 (s, 2H, H7,28), 8.11 (d,$^3J_{H,H}$ = 8.4 Hz, 4H, H10,12,23,27), 7.45–7.41 (m, 4H, H4,6,32,34), 7.31 (d,$^3J_{H,H}$ = 8.4 Hz, 4H, H9,13,24,26), 7.06, (d, $^3J_{H,H}$ = 8.4 Hz, 2H, H3,31), 6.98 (t, $^3J_{H,H}$ = 7.4 Hz, 2H, H5,33), 4.05 (s, 4H, H15,20), 0.31 (s, 12H, H16-19). ^{13}C NMR ($CDCl_3$, 100.16 MHz, δ, ppm): 166.6 (C14,21), 164.0 (C7,28), 161.2 (C2,30), 152.3 (C8,25), 133.7 (C4,32), 132.6 (C6,34), 130.8 (C10,12,23,27), 128.5 (C11,22), 121.1 (C9,13,24,26), 119.2 (C5,33), 118.9 (C1,29), 117.3 (C3,31), 58.2 (C15,20), − 0.8 (C16-19).

*4.5.3.2 Synthesis of the imine **3** derived from the diamine **1** and 3,5-dibromosalicylaldehyde*. To a stirred solution of diamine, **1**, (0.432 g, 1 mmol) in methanol/chloroform (1:2, v/v), 3,5-dibromosalicylaldehyde (0.567 g, 2 mmol) was added and the mixture was stirred at room temperature for 3 h. A red precipitate was formed. The product was filtered, washed with diethyl ether and then crystallised from chloroform (0.87 g, 91% yield). IR spectrum (KBr pellet), cm^{-1}: 3402 w, 3066 w, 2958 w, 2906 w, 1710 vs, 1703 vs, 1616 m, 1591 vs, 1550 m, 1502 w, 1446 s, 1427 m, 1413 m, 1384 m, 1357 m, 1313 vs, 1251 s, 1199 m, 1164 vs, 1110 s, 1055 s, 1014 m, 989 w, 945 w, 839 s, 798 s, 773 s, 738 m, 711 m, 690 s, 634 w, 603 w, 553 w, 538 w, 503 vw, 486 vw, 459 vw, 399 w.

^{1}H NMR ($CDCl_3$, 400.13 MHz, δ, ppm): 14.03 (s, 2H, OH), 8.56 (s, 2H, H7,28), 8.10 (d,$^3J_{H,H}$ = 8.4 Hz, 4H, H10,12,23,27), 7.80 (d, $^4J_{H,H}$ = 2.4 Hz, 2H, H4,32), 7.52 (d, $^4J_{H,H}$ = 2.4 Hz, 2H, H6,30), 7.30, (d, 4H, H9,13,24,26, overlap with solvent residual peak), 4.04 (s, 4H, H15,20), 0.30 (s, 12H, H16-19). ^{13}C NMR ($CDCl_3$, 100.16 MHz, δ, ppm): 166.4 (C14,21), 161.6 (C7,28), 157.3 (C2,34), 150.4 (C8,25), 138.7 (C4,32), 133.7 (C6,30), 131.0 (C10,12,23,27), 129.5 (C11,22), 121.2 (C9,13,24,26), 120.4 (C1,29), 112.3 (C3,33), 110.5 (C5,31) 58.4 (C15,20), − 0.8 (C16-19).

*4.5.3.3 Synthesis of the imine **4** derived from diamine **1** and 5-chlorosalicylaldehyde*. To a stirred solution of diamine, **1**, (0.432 g, 1 mmol) in methanol/chloroform (1:2, v/v), 5-chlorosalicylaldehyde (0.313 g, 2 mmol) was added and the mixture was stirred at room temperature for 3 h. A solid yellow precipitate was formed. The product was filtered, washed with diethyl ether and then crystallised from chloroform (0.66 g, 95% yield). IR spectrum (KBr pellet), cm^{-1}: 3373 w, 3060 vw, 2958 w, 2904 w, 1706 vs, 1618 m, 1600 s, 1562 s, 1517 w, 1504 w, 1479 s, 1431 w, 1415 m, 1384 m, 1357 m, 1317 vs, 1278 s, 1255 vs, 1170 s, 1118 s, 1072 s, 1014 m, 991 w, 979 w, 968 w, 925 w, 842 s, 817 s, 798 s, 785 s, 769 s, 727 m, 696 m, 671 w, 649 m, 636 w, 536 w, 516 w, 443 vw, 399 w.

^{1}H NMR ($CDCl_3$, 400.13 MHz, δ, ppm): 12.92 (s, 2H, OH), 8.57 (s, 2H, H7,28), 8.11 (d,$^3J_{H,H}$ = 8.4 Hz, 4H, H10,12,23,27), 7.40 (d, $^4J_{H,H}$ = 2.4 Hz, 2H, H6,34), 7.38 (dd, $^3J_{H,H}$ = 8.8 Hz, $^4J_{H,H}$ = 2.4 Hz, 2H, H4,32), 7.30, (d, 4H, H9,13,24,26, overlap with solvent residual peak), 7.01 (d, $^3J_{H,H}$ = 8.8 Hz, 2H, H3,31) 4.04 (s, 4H, H15,20), 0.30 (s, 12H, H16-19). ^{13}C NMR ($CDCl_3$, 100.16 MHz, δ, ppm): 166.5 (C14,21), 162.7 (C7,28), 159.7 (C2,30), 151.7 (C8,25), 133.5 (C4,32), 131.5 (C6,34), 130.9 (C10,12,23,27), 129.0 (C11,22), 123.9 (C1,29) 121.1 (C9,13,24,26), 119.6 (C5,33), 118.9 (C3,31), 58.3 (C15,20), − 0.8 (C16-19).

*4.5.3.4 Synthesis of the imine **5** derived from the diamine **1** and 3,5-di-tert-butyl-2-hydroxybenzaldehyde*. To a stirred solution of diamine, **1**, (0.432 g, 1 mmol) in methanol/chloroform (1:2, v/v), 3,5-di-*tert*-butyl-2-hydroxybenzaldehyde (0.468 g, 2 mmol) was added. The mixture was refluxed for 4 h, then the solvent mixture was slowly evaporated at room temperature, which resulted in the formation of yellow crystals (0.72 g, 83% yield). IR spectrum (KBr pellet), cm^{-1}: 3402 w, 2997 w, 2958 s, 2910 m, 2868 m, 1710 vs, 1649 m, 1618 s, 1602 s, 1577 vs, 1504 w, 1465 m, 1438 m, 1413 m, 1384 s, 1363 m,

1311 s, 1299 s, 1249 s, 1199 m, 1166 vs, 1114 s, 1056 s, 1016 m, 997 w, 983 w, 964 w, 931 vw, 879 m, 852 s, 839 s, 798 s, 769 s, 715 m, 696 m, 642 w, 619 vw, 588 vw, 534 vw, 513 w, 397 w, 379 vw.

^{1}H NMR ($CDCl_3$, 400.13 MHz, δ, ppm): 13.43 (s, 1H, OH), 8.68 (s, 1H, H15), 8.12 (d, $^3J_{H,H} = 8.4$ Hz, 2H, H18,20), 7.53 (d, $^4J_{H,H} = 2.4$ Hz, 1H, H4), 7.34 (d, $^3J_{H,H} = 8.4$ Hz, 2H, H17,21), 7.28, (d, $^4J_{H,H} = 2.4$ Hz, 1H, H6), 4.06 (s, 2H, H23), 1.52 (s, 9H, H12-14), 1.38 (s, 9H, H12-14), 0.31 (s, 6H, H24,25). ^{13}C NMR ($CDCl_3$, 100.16 MHz, δ, ppm): 166.8 (C22), 165.2 (C15), 158.4 (C2), 152.6 (C16), 140.8 (C5), 137.1 (C3), 130.9 (C18,20), 128.7 (C4), 128.2 (C19) 127.1 (C6), 121.1 (C17,21), 118.1 (C1), 58.2 (C23), 35.1 (C7), 34.2 (C11), 31.4 (C12-14), 29.4 (C8-10), −0.8 (C24,25).

CCDC-901925 (1), CCDC-901926 (2), CCDC-901927 (3), CCDC-901928 (4) and CCDC-901924 (5) contain the supplementary crystallographic data for this contribution. These data can be obtained free of charge via http://www.ccdc.cam.ac.uk/conts/retrieving.html (or from the Cambridge Crystallographic Data Centre, 12 Union Road, Cambridge CB2 1EZ, UK; fax: (+44) 1223-336-033; or deposit@ccdc.ca.ac.uk).

Supporting Information

Copies of FTIR, ^{1}H NMR, ^{13}C NMR, H,H-COSY, H,C-HMQC, and H,C-HMBC spectra for all key intermediates and final products; figures showing π−π stacking association for the compounds **2**–**5** are also enclosed.

Acknowledgements

This research was financially supported by European Regional Development Fund, Sectoral Operational Programme 'Increase of Economic Competitiveness', Priority Axis 2 (SOP IEC-A2-O2.1.2-2009-2, ID 570, COD SMIS-CSNR: 12473, Contract 129/2010-POLISILMET).

References

(1) (a) Sprung, M.A. *Chem. Rev.* **1940**, *26*, 297–338; (b) Patai, S. *The Chemistry of the Carbon–Nitrogen Double Bond;* J. Wiley & Sons, London, **1970**; (c) Calligaris, M.; Nardin, G.; Randaccio, L. *Coord. Chem. Rev.* **1972**, *7*, 385–403; (d) Yamada, S. *Coord. Chem. Rev.* **1999**, *190–192*, 537–555.

(2) (a) Layer, R.W. *Chem. Rev.* **1963**, *63*, 489–510; (b) Kolawole, G.A.; Patel, K.S. *J. Chem. Soc*. (Dalton Trans.) **1981**, 1241–1245; (c) Hancock, R.D.; Martell, A.E. *Chem. Rev.* **1989**, *89*, 1875–1914; (d) Garnovskii, A.D.; Nivorozhkin, A.L.; Minkin, V.I. *Coord. Chem. Rev.* **1993**, *126*, 1–69; (e) Cozzi, P.G. *Chem. Soc. Rev.* **2004**, *33*, 410–421.

(3) (a) Tümer, M.; Köksal, H.; Şener, M.K.; Serin, S. *Transition Met. Chem*. **1999**, *24*, 414–420; (b) Kumar, S.; Dhar, D.N.; Saxena, P.N. *J. Sci. Ind. Res.* **2009**, *68*, 181–187; (c) Arulmurugan, S.; Kavitha, H.P.; Venkatraman, B.R. *Rasayan J. Chem*. **2010**, *3*, 385–410.

(4) Spichiger-Keller, U. *Chemical Sesors and Biosensors for Medical and Biological Applications*; Wiley-VCH: Weinheim, 1998.

(5) Jungreis, E.; Thabet, S. *Analytical Applications of Schiff Bases*; Marcell Dekker: New York, 1969.

(6) Ibrahim, M.N.; Sharif, S.E.A. *E-J. Chem.* **2007**, *4*, 531–535, http://www.e-journals.net

(7) (a) Katsuki, T. *Coord. Chem. Rev.* **1995,** *140*, 189–214; (b) Gál, E.; Găină, L.; Lovász, T.; Cristea, C.; Silaghi-Dumitrescu, L. *Studia Universitatis Babeş-Bolyai Series Chemia* LIV **2009**, *4*, 17–24.

(8) (a) Basolo, F.; Hoffman, B.M.; Ibers, J.A. *Acc. Chem. Res*. **1975**, *8*, 384–392; (b) Leung, A.C.W.; MacLachlan, M.J.J. *Inorg. Organometal. Polym. Mater.* **2007**, *17*, 57–89.

(9) Govender, S. Structural and Physical Studies of Co(III) Salen Derivatives. M.Sc. Thesis., University of KwaZulu-Natal, Pietermaritzburg, **2007**, http://www.hdl.handle.net/10413/202

(10) Arun, V. Synthesis and Characterisation of New Transition Metal Complexes of Schiff Bases Derived From 3-hydroxyquinoxaline-2-carboxaldehyde and Application of Some of These Complexes as Hydrogenation and Oxidation Catalysts, PhD Thesis, Cochin University of Science and Technology, Kerala, India, **2009**, p. 1–36.

(11) Kianfara, A.H.; Zargarib, S.; Khavasic, H.R. *J. Iran. Chem. Soc.* **2010**, *7*, 908–916.

(12) Deshpande, S.; Srinivas, D.; Ratnasamy, P. *J. Catal.* **1999**, *188*, 261–269, and references therein.

(13) (a) Costamagna, J.; Vargas, J.; Latorre, R.; Alvarado, A.; Mena, G. *Coor. Chem. Rev.* **1992**, *119*, 67-88; (b) Sun, S.S.; Stern, C.L.; Nguyen, S.T.; Hupp, J.T.J. *Am. Chem. Soc*. **2004,** *126,* 6314-6326; (c) Matsumoto, K.;Saito, B.; Katsuki, T. *Chem. Commun.* **2007**, 3619–3627; (d) Whiteoak, C.J.; Salassa, G.; Kleij, A.W. *Chem. Soc. Rev.* **2012**,*41*, 622–631.

(14) (a) Canali, L.; Sherrington, D.C. *Chem. Soc. Rev.* **1998**, *28*, 85; (b) Bandini, M.; Cozzi, P.G.; Umani-Ronchi, A. *Chem. Commun.* **2002**, 919–927; (c) Yoon, T.P.; Jacobsen, E.N. *Science,* **2003**, *299*, 1691–1693; (d) Bailezao, C.; Garcia, H. *Chem. Rev.* **2006**, *106*, 3987–4043; (e) Feltham, H.L.C.; Brooker, S. *Coord. Chem. Rev.* **2009,** *253*, 1458–1475; (f) Zulauf, A.; Mellah, M.; Hong, X.; Schulz, E. *Dalton Trans.* **2010**, *39*, 6911–6935.

(15) Marcu, M.; Cazacu, M.; Vlad, A.; Racles, C. *Appl. Organomet. Chem.* **2003**, *17*, 693–700.

(16) Cazacu, M.; Marcu, M.; Vlad, A.; Rusu, Gh.I.; Avadanei, M. *J. Organomet. Chem.* **2004**, *689*, 3005–3011.

(17) Cazacu, M.; Marcu, M.; Vlad, A.; Toth, A.; Racles, C. *J. Polym. Sci. Part A – Polym. Chem.* **2003**, *1*, 3169–3179.

(18) Soroceanu, A.; Cazacu, M.; Shova, S.; Turta, C.; Kožišek, J.; Gall, M.; Breza, M.; Rapta, P.; Mac Leod, T.C.O.; Pombeiro, A.J.L.; Telser, J.; Dobrov, A.A.; Arion, V.B. *J. Inorg. Chem.* **2013**, 1458–1474.

(19) Vlad, A.; Turta, C.; Cazacu, M.; Rusu, E.; Shova, S. *Eur. J. Inorg. Chem.* **2012**, *31*, 5078–5084.

(20) Noll, W. In *Chemistry and Technology of Silicones*; Noll, W., Ed.; Academic Press Inc. (London) Ltd: New York, 1968.

(21) Fereday, A.; Goodgame, D.M.L.; Lickiss, P.D.; Rooke, S.J.; White, A.J.P.; Williams, D.J. *Inorg. Chem. Commun.* **2002**, *5*, 805–807.

(22) Di Iulio, C.; Jones, M.D.; Mahon, M.F.; Apperley, D.C. *Inorg. Chem.* **2010**, *49*, 10232–10234.

(23) Zhao, Z.; Cammidge, A.N.; Hughes, D.L.; Cook, M.J. *Org. Lett.* **2010**, *12*, 5138–5141.
(24) Issa, R.M.; Khedr, A.M.; Rizk, H. *J. Chin. Chem. Soc.* **2008**, *55*, 875–884.
(25) (a) Hodnett, E.M.; Dunn, W.J., *J. Med. Chem.* **1970**, *13*, 768–770; (b) Hodnett, E.M.; Mooney, P.D.J. *Med. Chem.* **1970**, *13,* 786; (c) El-Gamel, N.E.A *RSC Adv.* **2012**, *2*, 5870–5876.
(26) Wang, P.H.; Keck, J.G.; Lien, E.J.; Lai, M.M.C. *J. Med. Chem.* **1990**, *33*, 608–614.
(27) (a) Shi, L.; Ge, H.M.; Tan, S.H.; Li, H.Q.; Song, Y.C.; Zhu, H.L.; Tan, R.X. *Eur. J. Med. Chem.* **2007**, *42*, 558–564; (b) Belaid, S.; Landreau, A.; Djebbar, S.; Benali-Baitich, Q.; Bouet, G.; Bouchara, J.P.J. *Inorg. Biochem.* **2008**, *102*, 63–69; (c) Xu, S.P.; Shi, L.; Lu, P.G.; Fang, R.Q.; Zhu, H.L *J. Coord. Chem.* **2009**, *62*, 2048–2057; (d) Cheng, K.; Zheng, Q.Z.; Qian, Y.; Shi, L.; Zhao, J.; Zhu, H.L. *Bioorg. Med. Chem.* **2009**, *17*, 7861–7871.
(28) Cinarli, A.; Gürbüz, D.; Tavman, A.; Seher Birteksöz, A. *Bull. Chem. Soc. Ethiop.* **2011**, *25*, 407–417.
(29) da Silva, C.M.; da Silva, D.L.; Modolo, L.V.; Alves, R.B.; de Resende, M.A.; Martins, C.V.B.; de Fatima, A. *J. Adv. Res.* **2011**, *2*, 1–8.
(30) CrysAlis RED, Oxford Diffraction Ltd., Version 1.171.34.76, **2003**.
(31) Sheldrick, G.M. *Acta Crystallogr.* **2008**, *64*, 112–122.